Degenerate Germanium. I. Tunnel, Excess, and Thermal Current in Tunnel Diodes

DIETRICH MEYERHOFER, GEORGE A. BROWN, AND H. S. SOMMERS, JR.
RCA Laboratories, Princeton, New Jersey
(Received December 15, 1961)

The conduction processes in germanium tunnel diodes under forward bias are studied experimentally and compared with existing theories. Conductance is measured on an assortment of diodes with regrown *p-n* junctions, doped with known amounts of arsenic and gallium, in the temperature range 4.2° to 300°K. Capacitance is measured as a function of voltage at room temperature. The studies deal in particular with the temperature and composition dependence of the thermal current, of the peak tunnel current and peak voltage, and of the exponential component of the excess current. The thermal current varies as $\exp(eV/kT)$. At low temperature the potential barrier controlling it has an unexpected independence of the doping, a fact not easily understood in terms of minority carrier injection. At 300°K injection does occur as shown by the capacitance measurements. The peak tunnel current and voltage are found to agree quantitatively with Kane's theory of direct band-to-band tunneling for all tunnel junctions, covering a doping range from 3×10^{18} to $3\times10^{20}/\text{cm}^3$. The change of peak current with temperature is correlated with the variation of band-gap and Fermi level position. The excess current, which in some diodes has an exponential increase with bias for over half the band-gap voltage, is shown to be closely related to the peak current, in agreement with theory.

I. INTRODUCTION

THIS paper reports a comprehensive study of the conduction processes in abrupt *p-n* junctions of degenerate germanium under forward bias. Interest in the properties of narrow junctions has been growing, since the report of a negative resistance region in the current-voltage characteristic by Esaki.[1,2] Although several studies of particular aspects of the forward admittance have been performed, there has been no systematic investigation of the various conduction mechanisms and their inter-relationship. Such an investigation is of fundamental importance, because of the information it will give about changes in the band structure of degenerate materials and of the transport processes in degenerate junctions. We present here experimental results of a series of measurements of the forward admittance of germanium tunnel diodes with well controlled and known impurity concentrations over the temperature range from 4.2° to 300°K. An attempt to understand the implications of these results on the band gap of degenerate germanium and the correlations between the various recombination processes is presented in a companion paper by one of the authors,[3] which will be referred to as II.

The current-voltage characteristic of a tunnel diode under forward bias is composed of the three distinct regions of tunnel, excess, and thermal current. Figure 1 presents a typical example. The inserts depict the relative positions of the Fermi levels and the band edges, and the current flow mechanism for electron conduction. Analogous diagrams can be drawn for hole conduction.

Band-to-band tunneling has been studied in some detail in the reverse direction by Chynoweth *et al.*[4] and in the negative resistance region by Furukawa,[5] and qualitative agreement has been obtained with the simplified theory.[6] More sophisticated three-dimensional theories include the effect of phonons and ellipsoidal energy bands on the tunneling,[7,8] but none is yet sufficiently complete to give a good account of the shape of the *I-V* characteristic. Our studies have been confined to detailed measurements of the temperature and doping dependence of the current and voltage at the maximum.

The existence of the excess current was recognized

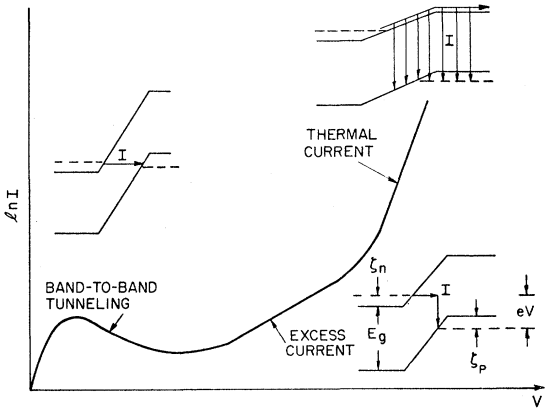

FIG. 1. Current-voltage characteristic of a degenerate *p-n* junction. Inserts show the relative positions of the bands and the paths of electron flow for three principal components of current. E_G is the thermal gap; ζ_n and ζ_p are the penetrations of the Fermi levels into the conduction and valence bands.

[1] L. Esaki, Phys. Rev. **109**, 603 (1958).
[2] L. Esaki, *Solid State Physics in Electronics and Telecommunications* (Academic Press Inc., New York, 1960), Vol. I, p. 514.
[3] H. S. Sommers, Jr., Phys. Rev., **124**, 1101 (1961). This paper will be referred to as II.
[4] A. G. Chynoweth, W. L. Feldman, C. A. Lee, R. A. Logan, G. L. Pearson, and P. Aigrain Phys. Rev. **118**, 425 (1960).
[5] Y. Furukawa, J. Phys. Soc. Japan **15**, 730 (1960).
[6] W. Franz, *Handbuch der Physik*, edited by S. Flügge (Springer-Verlag, Berlin, 1956), Vol. 17, p. 155.
[7] L. V. Keldysh, J. Exptl. Theoret. Phys. (USSR) **33**, 994 (1957); **34**, 962 (1958) [translation: Soviet Phys.—JETP **6**, 763 (1958); **7**, 665 (1958), respectively].
[8] E. O. Kane, J. Appl. Phys. **32**, 83 (1961).

TABLE I. List of diodes investigated and their properties in the band-to-band tunneling region. J_p and V_p are measured at 4.2°K, I_p/C at 300°K.

Group	No. of units	Impurity concentration n (10^{19} cm^{-3})	Impurity concentration p (10^{19} cm^{-3})	Peak current I_p/C (ma/pf)	Peak current J_p (amp/cm^2)	Peak current rms deviation (%)	Peak voltage V_p (mv)	Peak voltage rms deviation (mv)
N-1	3	3.0	1		51	40	37	3
N-2	1	3.0	3.5		230		43	
N-3	4	1.5	8		38	10	63	3
N-4	4	2.8	8		220	10	64	3
P-1	5	4.5	0.084					
P-2	5	4.5	0.132					
P-3	4	4.5	0.344	8×10^{-5}	0.13	40	32	3
P-4	4	4.5	0.511	1.3×10^{-3}	2.4	30	39	2
P-5	4	4.5	1.08	2.6×10^{-2}	68	25	41	2
P-6	5	4.5	2.0	0.23	533	9	49	3
P-7	4	4.5	2.8	0.64	1420	18	54	3
P-8	12	4.5	5.2	1.76	3560	34	74	9
P-9	3	4.5	5.5	1.49	3800	30	86	10
P-10	3	4.5	10.0	4.2	7640	8	105	10
P-11	3	4.5	12.6	3.8	6600	24	100	10
P-12	4	4.5	23.8	10.4	16 000	38	125	15

by Yajima and Esaki,[9] who suggested it was an indirect tunneling between the bands involving centers in the energy gap. This model has been studied phenomenologically by Chynoweth *et al.*,[10] who found good agreement between their theory and the results of a detailed study of silicon junctions. Our studies concentrate on the prominent feature of the excess current in high-quality germanium tunnel diodes, the component which increases exponentially with bias voltage.

The exponential excess and thermal currents both have an exponential I-V characteristic, but they can be readily distinguished from each other by the great difference in their change with temperature, the excess current being nearly temperature-independent. Our most significant contribution is the study of the thermal current, whose properties in heavily doped junctions have not yet been reported in the literature. In junctions of nondegenerate germanium, it is generally accepted[11] that the thermal current is carried by minority carrier injection into the base of the diode, as described by Shockley.[12] However, a simple extrapolation of his treatment to degenerate material does not describe our results. In particular, the experiments show that the height of the barrier to thermal current becomes nearly independent of the position of the Fermi level at high dopings. A model based on junction recombination, presented in II, seems to explain both our results and the optical emission spectrum of Pankove.[13]

The capacitance was measured as a function of forward bias for all diodes with high enough impedance to be balanced on our bridges. At low bias, the transition capacitance varied as expected for an abrupt junction,[12] while at extreme forward bias we observe a pair-storage capacitance[12]; no capacitance associated with the excess current was detected.

The experimental procedures are given in the next section. Then, the experimental results of each component of current are presented, compared with data in the literature, and interpreted in terms of existing theories. General conclusions are summarized in the final section.

II. EXPERIMENTAL

A. Diode Fabrication

All diodes were fabricated by the solution regrowth technique developed in this laboratory by Nelson.[14] The surface of a heavily doped wafer of germanium of known concentration is dissolved in a solution of Ge and the complementary dopant, in an appropriate solvent. A new layer is grown on the surface by lowering the temperature. The junction lies at the interface of the original and regrown layers. The dopants were always As and Ga. As long as diffusion in the solid is negligible, this process should result in abrupt junctions with constant impurity concentration on both sides. A mesa is then developed by lapping or etching, and the diode is mounted in an appropriate high-frequency enclosure.

The various groups of diodes investigated are described in Table I. The donor and acceptor concentrations, columns 3 and 4, are measured values in the bulk and in the regrown layers. Groups N-1 and N-2 are from groups of n-on-p diodes made early in the program when the details of processing were not completely known. Groups N-3 and N-4 are p-on-n diodes. The regrowth solution was In with 1% Ga and

[9] T. Yajima and L. Esaki, J. Phys. Soc. Japan **13**, 1281 (1958).
[10] A. G. Chynoweth, W. A. Feldman, and R. A. Logan, Phys. Rev. **121**, 684 (1961).
[11] See, for example, W. Shockley, *Electrons and Holes in Semiconductors* (D. Van Nostrand Company, Inc., Princeton, New Jersey, 1950), p. 91.
[12] W. Shockley, Bell System Tech. J. **28**, 435 (1949).
[13] J. I. Pankove, Phys. Rev. Letters, **4**, 20 (1960).
[14] N. H. Ditrick and H. Nelson, RCA Engineer, 1960 (unpublished).

the growth temperature decreased from a maximum 520° to 460°C in approximately 4 min. Under these conditions the As should diffuse more than 200 Å from the base into the regrown layer.[15] The junction width for tunneling is the distance between the classical turning points, i.e., the points where the Fermi level goes through the band edge. This width is only about 80 Å for these diodes in spite of the diffusion; the concentration of As in the transition region is calculated to be between 0.5 and 0.7 times the bulk concentrations. (The regrown p-type layer is much more heavily doped than the base.) The junction width for tunneling can, therefore, be calculated approximately by assuming an abrupt junction with an average donor concentration of 0.6 times the bulk value given in Table I. The junctions of groups N-3 and N-4 were planar and the regrown layers of excellent crystallinity and uniform doping. Consequently, it was possible to measure the concentration of acceptors, both electrically and chemically.

The P groups of diodes were grown especially for this investigation. Identical n-type layers were grown on a large number of different p-type crystals. The solution used was a Pb-Sn mixture with 1% As and was cooled from 410°C, at which temperature the diffusion length of As was always less than the junction width.[15] The junctions showed excellent reproducibility, as can be seen from the ratio of peak tunnel current to zero bias capacitance (I_p/C). This quantity is a very sensitive indicator of the carrier concentrations adjacent to the junction because of the exponential dependence of the tunneling on the internal field, while at the same time it is independent of the junction area, which is difficult to measure. The data, Table I, column 5, is graphed against the hole concentration in Fig. 2. The vertical deviations shown are the rms variations for junctions made from the same crystal. The fact that the points lie on a smooth curve is an indication of the degree of control of the doping of the Pb-Sn-As regrown layer.

The As concentration of the regrown layer at the junction could not be accurately determined because of a slow variation with depth. Approximate values were deduced from a comparison of chemical analysis, sheet resistance, and change of capacitance with voltage. All these measurements were consistent and gave the result that $n=(4.5\pm1.0)\times10^{19}$ cm^{-3} at the junction of the P diodes.

The cross-sectional area A of all the junctions was determined from the known impurity concentrations (Table I) and the measured voltage dependence of the transition capacitance, C_{tr}, according to the equation for an abrupt junction:

$$C_{tr}/A=(e\epsilon/2)^{\frac{1}{2}}n^{*\frac{1}{2}}(V_D-V)^{-\frac{1}{2}}, \quad (1)$$

where

$$n^*=np/(n+p) \quad (2)$$

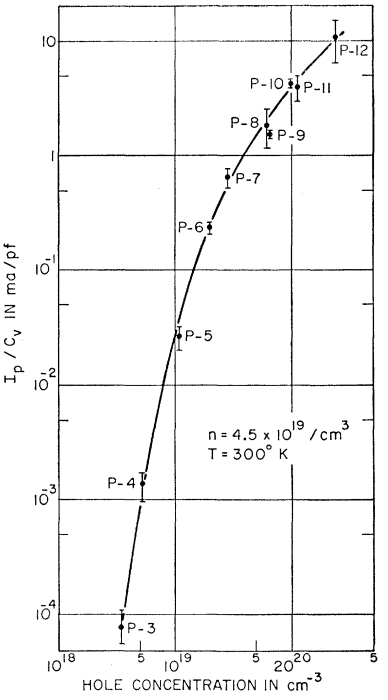

FIG. 2. Band-to-band tunneling; ratio of peak current to capacitance vs hole concentration for junctions with regrown n layers. The vertical bars are the statistical deviations within each group of diodes.

is the reduced concentration. A is the junction area, V_D the diffusion potential, n and p the electron and hole concentrations, e the fundamental charge, and ϵ the dielectric constant; mks units are used.

B. Measurements of Diode Characteristics

The experimental work consisted of measuring current, conductance, and capacitance as functions of voltage and temperature at dc or low frequency. To perform any of these measurements in the negative resistance region, it is necessary to stabilize the diode with a small parallel resistance, which requires a low lead inductance.[16,17] When stabilization is not possible, studies can be made only in the positive resistance regions. A number of different low-impedance jigs were used. One which can be used conveniently at low temperatures is shown in Fig. 3. The diode and a temperature independent deposited carbon resistor of similar size are mounted between the two solid cylindrical contact blocks. Electrical contacts to the upper block are made by gold-plated screws which are connected to the top of the sample holder with insulating rods. It is, therefore, possible to disconnect both the diode and the resistor from the circuit while they are at the testing temperature, which permits calibration of the resistor and measurement of the diode resistance. The thermocouple is located next to the diode. The temperature measurements were accurate to 1°K, the largest difference measured between the two contact blocks in a test run.

[15] W. Dunlap, Phys. Engineer, 1960 (unpublished).

[16] H. S. Sommers, Jr., Proc. Inst. Radio Engrs. **47**, 1201 (1959).

[17] A. M. Goodman, Rev. Sci. Instr. **31**, 286 (1960).

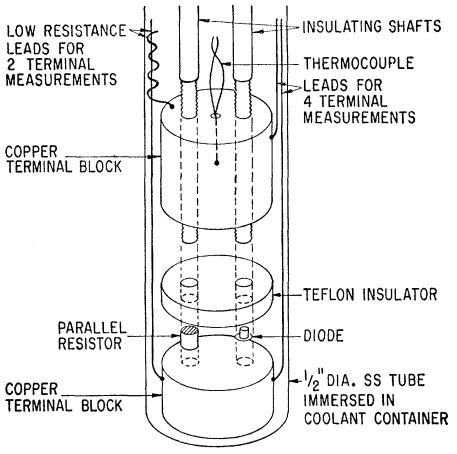

FIG. 3. Low-impedance jig for use in cryostat. Expanded view showing position of diode, shunting resistor, and releasable clamping screws. Diode and resistor can be measured alone or together without removing from cryostat.

The I-V and G-V characteristics were either measured point by point with dc or pulses or continuously recorded by using a 1000 cps ac technique.[17] Alternatively, the conductance was measured on a uhf bridge. The accuracy of both voltage and current measurements was 1%, or better. Voltage values were corrected for series resistance.

Capacitance was measured as a function of bias voltage with an admittance bridge. For units with conductance less than 1 millimho, a 1 Mc/sec precision bridge was used (1% accuracy); diodes between 1 and 100 mmho were measured on a Wayne Kerr uhf admittance bridge at 30 Mc/sec (±1 pf). In either case, the measured values had to be corrected for lead inductance, which ranged from 200 to 400 ph depending on the mount; for series resistance; and for case capacitance of less than 1 pf. These corrections become large for large values of shunt conductance, so that high-accuracy measurements were limited to low-current diodes and to small forward voltages.

III. RESULTS AND ANALYSIS

A. Band-to-Band Tunneling

Behavior at $T=0$

The theory of the band-to-band tunneling current is simplest at $T=0$, where the Fermi function becomes a step function and the integrals over the energy simplify considerably. Therefore, the data near this temperature will be presented first. The values J_p and V_p at the peak of the tunneling current, measured at 4.2°K, are listed in Table I (columns 6 and 8). The values of the groups N-2 and N-4 are extrapolated from higher temperatures in accordance with the results of the following section. A series resistance correction was applied to V_p, where necessary. In the most lightly doped group of diodes, where the excess current was comparable to the tunnel current, the excess current has been subtracted to give I_p. The extrapolation of the excess current was somewhat arbitrary and reduced the accuracy of the results of the group P-3.

The values listed in Table I are averages over each group of diodes, while the rms deviations are the measured variations from diode to diode in the group. The uncertainties in the measurements are considerably smaller, averaging 5 to 10% for both current and voltage. The measurements were always reproducible to within 2%. The additional scatter is probably due to variations in the doping, which has a strong effect on the tunneling.

The data may be compared most conveniently with the theory of Kane[8] who evaluated the general integrals for the Esaki effect[7] for a particular semiconductor model. He used the band structure of a typical III-V compound, i.e., the conduction and valence band extrema at the same point in k space. This does not in general apply to Ge, but in the case of tunnel diodes of Ge with As doping, the transition has been observed to occur without phonon assistance.[18] The momentum selection rules apparently are changed by the heavy As concentration. Consequently, it seems reasonable to apply Kane's calculation for the direct transition to these diodes using the value of the thermal gap. The other major assumptions made in the calculation are that the junction field F is constant and that the junction is abrupt with reduced concentration n^*. The tunneling current density in mks units is then

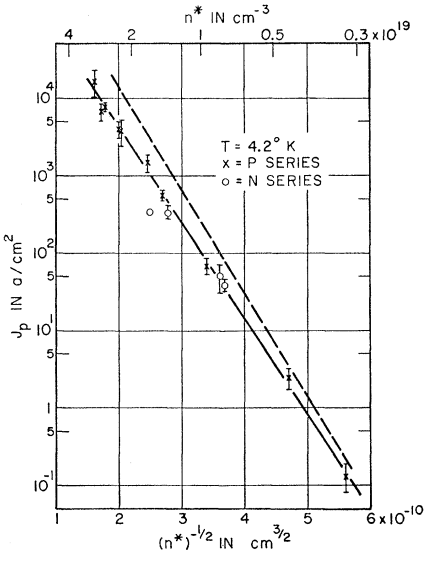

FIG. 4. Band-to-band tunneling. Current density as a function of reduced doping. The broken curve is calculated from Eq. (3) with no adjustable parameters. J_p is the current density at the peak; n^* is the reduced doping.

[18] N. Holonyak, Jr., I. A. Lesk, R. N. Hall, J. J. Tiemann, and H. Ehrenreich, Phys. Rev. Letters 3, 167 (1959).

$$J_t=\frac{em^*}{18\hbar^3}\frac{\bar{E}_\perp}{2}D\exp\left\{-\frac{\pi m^{*\frac{1}{2}}E_G^{\frac{3}{2}}}{2\sqrt{2}\hbar\bar{F}}\right\},$$

$$\bar{E}_\perp=(\sqrt{2}/\pi)(\hbar\bar{F}/m^{*\frac{1}{2}}E_G^{\frac{1}{2}}),$$

$$\bar{F}=(e^3/2\epsilon)^{\frac{1}{2}}n^{*\frac{1}{2}}V_D^{\frac{1}{2}}. \quad (3)$$

The diffusion potential V_D is approximately equal to E_G, the band gap, which gives the familiar exponential factor $(m^{*\frac{1}{2}}n^{*-\frac{1}{2}}E_G)$ for tunnel diodes; m^* is the effective mass for tunneling. The quantity D is an overlap integral which determines the shape of the I-V characteristic. It has the dimensions of voltage and depends on the depth of penetration of the Fermi levels into the energy bands, ζ_n and ζ_p. Its value at the current maximum is approximately equal to the magnitude of the peak voltage and does not vary much with doping for our diodes. The other quantities have their usual meaning.

J_p is plotted in Fig. 4 as a function of $n^{*-\frac{1}{2}}$. For diode groups N-3 and N-4, the donor concentrations corrected for diffusion have been used in calculating n^*. Each point represents the average current density for all similar junctions; the vertical line represents the root mean square fluctuation about the average. The theoretical curve of Eq. (3), with $E_G=0.745$ ev, $m^*=0.06m_0$ (reduced mass of electrons and light holes), is shown as the dashed line. The agreement is seen to be very good, both as to the slope of the exponential and as to the absolute value. This is interpreted as additional evidence that the transition is allowed.

A closer agreement between theory and experiment can not be expected due to the approximations of the calculation, particularly the constant field approximation and the neglect of the change of field with bias.

A similar set of measurements was performed by Furukawa[5] at room temperature. His junctions were formed by alloying in a controlled fashion on n-type crystals of known carrier concentration. Comparison of his peak current densities (Fig. 2 of reference 5) with our room temperature values shows the same exponential function, but his densities are a factor 40 lower than in the present case. A possible reason for this discrepancy is that diffusion of the As during his alloying process gave a decreased carrier concentration at the junction. A third set of measurements over a more limited range of concentration performed by Glicksman *et al.* on a set of diodes similar to our P diodes[19] agreed well with Fig. 4.

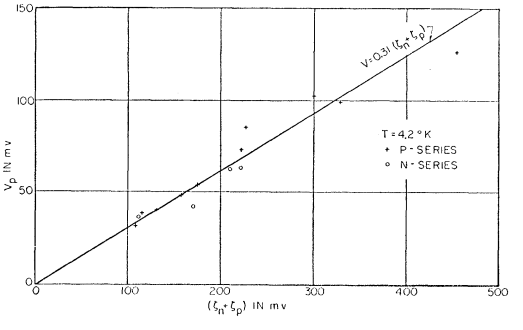

FIG. 5. Band-to-band tunneling. Voltage at the peak vs the sum of the Fermi level penetrations. ζ_n and ζ_p are the penetrations of the Fermi levels into the conduction and valence bands.

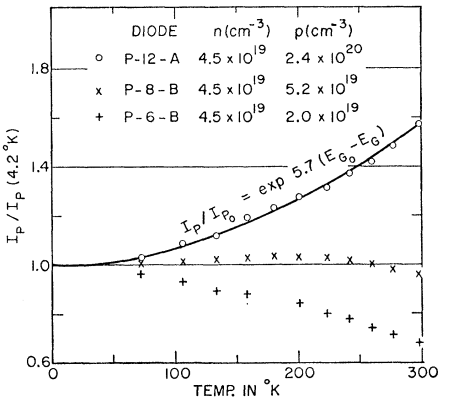

FIG. 6. Band-to-band tunneling. The temperature dependence of the peak current for three representative diodes. p is the hole concentration in the starting wafer; n is the electron concentration in the regrown layer.

The voltage at the peak, V_p, is given by Eq. (3) as the voltage where D is a maximum. For $\zeta_{\max}>2\zeta_{\min}$ (the larger and smaller of ζ_n and ζ_p, respectively) Eq. (3) is a flat-topped curve, centered between $\zeta_{\min}$ and $\zeta_{\max}$, for all values of $\bar{E}_\perp$. We expect $\bar{F}$ to decrease with applied bias so that the actual curve will not be flat-topped, but have a maximum at $V_p=\zeta_{\min}$ or slightly less. For $\zeta_{\max}<2\zeta_{\min}$ D always has a maximum which depends on the relative values of eV_p, $\zeta_{\min}$, and $\bar{E}_\perp$. However the maximum always falls between $\frac{1}{3}(\zeta_{\min}+\zeta_{\max})$ and $\zeta_{\min}$. The experimental values of V_p are shown in Fig. 5 as function of $(\zeta_n+\zeta_p)$. They closely fit a curve $V_p=\frac{1}{3}(\zeta_n+\zeta_p)$ over the entire range of doping, independent of whether $\zeta_{\max}$ is larger or smaller than $2\zeta_{\min}$. It is therefore apparent that Kane's theory of the shape of the I-V characteristic only qualitatively describes diodes of germanium. The direct dependency of V_p on the sum of the Fermi level penetrations does agree with the simple model proposed by Esaki.[1] It is not consistent with the suggestion of Logan *et al.*,[20] based on studies of silicon, that the bands uncross at a fixed voltage.

Temperature Dependence

The tunnel current is expected to vary only slowly with temperature. The measured dependence is shown in Fig. 6, where the normalized peak current is plotted against temperature for a representative diode from each of 3 groups. To explain the observed behavior we

[19] R. Glicksman and A. Blicher (private communication).
[20] A. R. Logan, W. N. Augustyniak, and J. F. Gilbert, J. Appl. Phys. **32**, 1201 (1961).

rewrite Eq. (3) as:

$$J_p = \text{const}\, n^{*-\frac{1}{2}} D_{\max} \exp\{-\beta m^{*\frac{1}{2}} n^{*-\frac{1}{2}} E_G\}. \quad (4)$$

There are 2 terms that influence the temperature behavior, $(m^{*\frac{1}{2}}E_G)$ and D. The negative value of $\partial E_G/\partial T$ means that the first term gives I_p a positive temperature coefficient. D will be essentially constant as long as ζ_n and ζ_p are large compared with kT. At higher temperatures the Fermi levels approach the band edges, an effect which reduces D. A number of attempts which have been made to calculate D (or some similar overlap integral including density of states)[21] include approximations that yield only a qualitative answer. We do know that in the high temperature limit the material is no longer degenerate and D vanishes. Hence, this effect by itself would give I_p a negative temperature coefficient.

The most heavily doped diodes (P-12) have $\zeta_n = 83$ mv, $\zeta_p = 371$ mv at $T = 0°$K. Since for this doping D should be unchanged until close to room temperature, its entire temperature dependence is due to the exponential term, and, therefore, to the change of the band gap E_G.[22] We find that diode P-12-A obeys this prediction if we take $\beta m^{*\frac{1}{2}} n^{*-\frac{1}{2}} = 5.7$ ev^{-1}, which yields the solid line in Fig. 6. A similar result was found with the other diodes of this group, P-12-B and P-12-C, which were studied at several temperatures. The average value of $\beta m^{*\frac{1}{2}}$ for the three junctions is 3.6×10^{10} cm$^{-\frac{3}{2}}$ ev^{-1}. This compares well with the value of 3.1×10^{10} cm$^{-\frac{3}{2}}$ ev^{-1} obtained from the slope of the $\ln I_p$ vs $n^{*-\frac{1}{2}}$ graph (Fig. 4), using $E_G = 0.74$ ev at 4.2°K, showing that the barrier penetrability of Eq. (4) has the correct dependence on temperature and doping.

In the more lightly doped diodes, the drop of D with increasing temperature reduces J_p below the value given by the exponential (Fig. 6). This change in the temperature behavior was pointed out by Longo,[23] and then studied over a limited temperature range by Allison[24] and Blicher *et al.*[25] The behavior is summarized in Fig. 7, where $J_p(300°\text{K})/J_p(4.2°\text{K})$ is plotted vs $(\zeta_n+\zeta_p)$ for all diodes measured. This shows the change from positive to negative temperature coefficient with doping. The behavior of the exponential part of Eq. (4) is also shown (dashed line) and the strong deviation due to the D term can be seen clearly. Other values of $J_p(300°\text{K})/J_p(4.2°\text{K})$ for germanium found in the literature[1,2,9,10,25] also fall on the curve of Fig. 7.

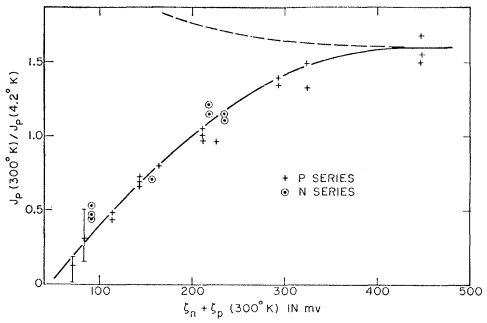

FIG. 7. Band-to-band tunneling. Ratio of peak current at 300°K to peak current at 4.2°K vs the sum of the Fermi level penetrations. The solid curve is a visual fit to the data. The dashed curve is the change expected from the temperature variation of the band gap. J_p is the current density at the peak; ζ_n and ζ_p the penetrations of the Fermi levels into the conduction and valence bands.

The value of peak voltage varies only slightly with temperature, due to the variation of $\frac{1}{3}(\zeta_n+\zeta_p)$. It increases a few percent from room temperature to 0°K, as expected for our diodes.[26] The variation is too small to warrant a detailed investigation.

Discussion

The behavior of the peak current with doping and with temperature is well predicted by the theory of the direct transition (Eq. 3). One of the assumptions in the derivation is that the band structure is similar to that of pure material except for a possible change in the effective mass. The quantitative agreement suggests that the gross features of the bands near the forbidden gap are unchanged, i.e., the energy dependence of the density of states is approximately the same as in pure material. In addition, no large change in effective mass (>20%) is observed, either with concentration or temperature, which agrees with the observations of Spitzer *et al.*[27]

B. Thermal Current Region

Voltage Dependence

At large forward biases, the conductance is always dominated by thermal current, that is, by a flow of carriers over some sort of a potential barrier. Consequently, it should depend on voltage as $\exp(eV/akT)$, with $1 \leqslant a \leqslant 2$ in most common cases.[28,29] The exact relationship between thermal current, voltage, and temperature was investigated for junctions covering all concentration ranges. The result for a typical diode is shown in Fig. 8. The solid curves are the raw data and must be corrected for series resistance, r, which is assumed to be independent of current. The constancy of r can be verified at 4.2°K, where the exponential curve is so steep that only the series resistance is observed (Fig. 8).

[21] C. W. Bates, Jr., Phys. Rev. **121**, 1070 (1961); T. P. Brody and R. H. Boyer, Solid State Electr. **2**, 209 (1961).
[22] G. G. Macfarlane, J. P. McLean, J. E. Quarrington, and V. Roberts, Phys. Rev. **108**, 1377 (1957).
[23] T. A. Longo, Bull. Am. Phys. Soc. II **5**, 160 (1960).
[24] J. Allison (private communication).
[25] A. Blicker, R. M. Minton, and R. Glicksman, Proc. Inst. Radio Engrs. **49**, 1428 (1961).
[26] R. P. Nanarati, Proc. Inst. Radio Engrs. **48**, 349 (1961).
[27] W. G. Spitzer, F. A. Trumbore, and R. A. Logan, J. Appl. Phys. **32**, 1822 (1961).
[28] C. T. Sah, R. N. Noyce, and W. Shockley, Proc. Inst. Radio Engrs. **45**, 1228 (1957).
[29] W. Shockley and R. Henley, Bull. Am. Phys. Soc. **6**, 106 (1961).

TABLE II. Characteristics of the thermal current: V_{2000} is the voltage at which the current density is 2000 amp/cm². τ is the lifetime calculated from storage capacitance.

Diode	4.2°K $V_{2000}=\phi$ (mv)	77°K V_{2000} (mv)	300°K V_{2000} (mv)	τ (nsec)	$Eg+\zeta_{min}$ (mv)	Eg (mv)
N-1-*A*	735	710	510		643±50	610±50
N-1-*B*	731	709	499		632±50	599±50
N-1-*C*	694	721	491		624±50	591±50
N-2-*A*	···	711	428		532	577
N-3-*A*	736	721	547	2	633	608
N-3-*B*	740	721	537	3	623	598
N-4-*A*	···	720	529		632	580
N-4-*B*	···	717	531		634	582
P-1-*A*	737	718	527		643	691
P-1-*B*	738	713	507	1.4	623	671
P-2-*A*	746	722	490	0.5[a]	618	658
P-3-*A*	737	697	478	0.6	634	641
P-3-*B*	735	741	520	0.7[a]	676	683
P-4-*A*	730	700	499		665	657
P-5-*A*	670	663	475		660	624
P-5-*B*	637	635	···		···	···
P-5-*C*	709	681	···		···	···
P-6-*A*	731	702	485		645±40	622
P-6-*B*	730	···	488		650±40	625
P-7-*A*	735	716	499		665±50	631
P-8-*A*	737	710	495		670±55	605±15
P-8-*B*	728	710	493		670±50	605±15
P-9-*A*	725	712	502		670±60	610±20
P-9-*B*	740	···	492		670±60	600±20
P-10-*A*	728	701	503		655±50	580±50
P-10-*B*	730	698	510		660±50	585±50
P-11-*A*	735	···	525		660±40	600±40
P-11-*B*	740	720	494		655±40	585±40
P-12-*A*	730	···	512		670±40	600±40
P-12-*B*	730	693	···			

[a] Measured by R. Cohen (reference 36).

Figure 8 shows in detail how r is determined at 300°K. Only the one value $r=0.12$ ohm gives a good exponential relationship; this has a logarithmic slope of 36.5 ev^{-1} ±5%. A small correction for excess current will increase this value by at most 1 ev^{-1}. For all diodes the measured slopes at 300°K fall within ±10% of $e/kT=39.2$ ev^{-1}. At 195°K the slope can again be determined with reasonable accuracy, and the values average about 10% less than $e/kT=60$ ev^{-1}. At 77°K the accuracy of this procedure is considerably reduced and the uncertainty becomes approximately 25%; the average value of the slopes is 0.8 e/kT. The deviation from e/kT is still within the experimental uncertainty. At 4.2°K, the slope is too steep to measure.

In some of the junctions the excess current is considerably larger than in *N*-1-*B* (Fig. 8), and it is difficult to separate the excess from the thermal current. In those cases, it was assumed that $I_{\text{thermal}} \propto \exp(eV/kT)$ and the measured $(I-V_m)$ characteristic was fitted by machine calculation to the equation

$$I=A_1e^{\sigma(V_m-Ir)}+A_2e^{(e/kT)(V_m-Ir)}. \quad (5)$$

The first term is the exponential excess current,[10] and the second the thermal current. In all cases satisfactory fits were obtained, giving unique values of the parameters σ, r, A_1, and A_2.

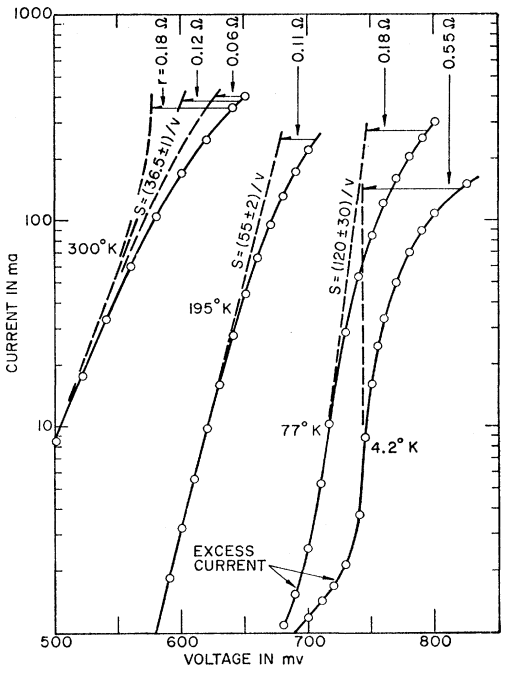

FIG. 8. Thermal current at high bias. Circles are raw data. Correction for series resistance r yields the dashed lines. "s" is the logarithmic derivative of the current deduced from the slopes of the dashed lines. Diode *N*-1-*B*, layer with $n=3\times10^{19}$/cm³ regrown on wafer with $p=1\times10^{19}$/cm³.

The dissipative resistance is not completely Ohmic, for the resistance in the reverse direction is generally somewhat higher than under extreme forward bias. The reduction of resistance does not seem to be due to either minority carrier injection or heating, for it is independent of current level as well as of pulse length for pulses from 10 μsec to dc. This suggests that the contacts or regions external to the junctions are not completely Ohmic. The resistance found in the forward direction was used for correcting all the data. As a rule, it was close to the calculated spreading resistance. Typical values are 0.1–1.0 ohm.

In Table II we have tabulated the measurements of the thermal current by listing values of V_{2000} for each diode, where V_{2000} is the forward voltage at which the current density, due to thermal current, is 2000 amp/cm². It turns out that this is a convenient value of current density for all the diodes, being in a region where the combined correction for series resistance and excess current is least troublesome. The estimated experimental errors are ±(5–10) mv at 4.2°K, ±10 mv at 77°K, and ±20 mv at 300°K. Since within the accuracy of our measurements the thermal current changes with voltages as $\exp(eV/kT)$, Table II defines our results for the thermal current at all voltages and temperatures.

Current Flow at Low Temperatures

At 4.2°K the thermal current is such a steep function of voltage that the barrier height, ϕ, can be determined

regardless of the model of recombination. In fact $\phi = V_{2000}$, the maximum estimated error in ϕ due to this approximation being $(+0, -10)kT = (+0, -5)$ mv. The striking result in Table II is that at 4.2°K, ϕ is essentially independent of diode and doping. Furthermore the values are only 5 to 20 mv less than the known band gap of pure Ge.[22] The only exceptions to this rule are N-1-C and group P-5. P-5-A was examined under a microscope and the junction was found to be structurally defective; our experience indicates that the other members of this group probably have the same defective junctions since they came from the same regrown wafer. The barrier height can, consequently, be considered constant to first order for good degenerate Ge diodes.

At 77°K, V_{2000} is again surprisingly constant, with most of the values falling between 695 and 725 mv. Again, this points to a constant barrier height.

Discussion

The discovery that the barrier height at low temperatures is independent of the doping in diodes of degenerate germanium was not expected on the basis of conventional theory. It has important implications about the effect of heavy doping on the band structure of germanium. Suggestions that have been proposed to account for it are:

(1) A narrow band of impurity states at the band edge has so perturbed the density of states that the Fermi level never penetrates an appreciable distance into the allowed band.[30,31] This explanation is inconsistent with the measurements of the effective mass of degenerate Ge,[27] with experience with InSb,[32] and, in fact, with the existence of the Esaki effect.[1]

(2) The energy gap has shrunk with doping in such a way that the Fermi level remains at a distance from the minority carrier band which is independent of doping.[33] This seems unlikely because of the reflection measurements of Cardona and Sommers[34] on p-type Ge and because of the nature of the thermal current, as discussed at length in II.

(3) The band structure is essentially unchanged by the heavy doping but the thermal current at low temperature is all carried by junction recombination.[28] As shown in II, this mode of current flow seems to be logically required on general grounds; for it, the barrier height cannot exceed the band gap. The particular model developed in II interprets the barrier height as the thermal gap, which then has shrunk by about 30 mv at the highest doping. This small change can be accounted for by the spreading of the impurity band of the donors and acceptors.[35]

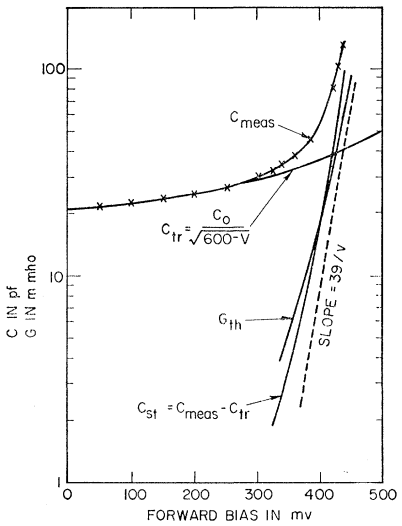

FIG. 9. Capacitance and conductance at high forward biases. C_{meas} is the measured capacitance, C_{tr} the transition capacitance extrapolated from low bias according to the law for an abrupt junction, and C_{st} and G_{th} the injection capacitance and conductance. The broken line is drawn with the slope e/kT. Diode N-3-B, layer with $n = 1.5\times10^{19}$/cm³ regrown on wafer with $P = 8\times10^{19}$/cm³.

Lifetime and Barrier Height at Room Temperature

At room temperature kT is of the order of ζ_{np} for most junctions. Consequently, minority carrier injection will become an important or dominant part of the thermal current. This current obeys the equation,[12]

$$J_{inj} = (ekT)^{\frac{1}{2}}\mu_n^{\frac{1}{2}}\tau_n^{-\frac{1}{2}}N_c \exp[eV - (E_G+\zeta_p)/kT], \quad (6)$$

for electron injection into the p-type side with a corresponding term for hole injection into the n-type side. μ_n and τ_n are the electron mobility and lifetime in the p-type material and N_c the effective density of states in the conduction band.

To evaluate Eq. (6) for $\phi = E_G+\zeta_p$, it is necessary to know τ_n (and τ_p, the hole lifetime). Lifetimes are very short in these heavily doped materials and cannot be determined by conventional means. However, the lifetime in the base region can be calculated from the junction capacitance at far forward bias provided the capacitance is dominated by pair storage, a condition applying when the ratio of conductance to capacitance becomes independent of bias voltage. Then the minority carrier lifetime is[12]

$$\tau = 2C_{st}(V)/G_{th}(V), \quad (7)$$

where $C_{st}(V)$ is the pair storage capacitance and $G_{th}(V)$ the conductance due to thermal injection.

Our technique permitted measurement of capacitance only when the junction conductance was less than 0.1 mho, so but a few diodes could be studied in this way. Even for these, the results are accurate only to

[30] J. I. Pankove, Ann. Phys. (Paris) **6**, 331 (1961).
[31] T. P. Brody, J. Appl. Phys. **32**, 746 (1961).
[32] E. Burstein, Phys. Rev. **93**, 632 (1954).
[33] J. I. Pankove, Phys. Rev. Letters **4**, 454 (1960).
[34] M. Cardona and H. S. Sommers, Jr., Phys. Rev. **122**, 1382 (1961).
[35] W. Baltensperger, Phil. Mag. **44**, 1355 (1953); E. M. Conwell, Phys. Rev. **103**, 51 (1956).

an order of magnitude, because of the large extrapolations needed to deduce C_{st} and G_{th} at a common bias voltage. A typical measurement of capacitance is shown in Fig. 9, diode N-3-B, in which the measured values of junction capacitance at various biases (C_{meas}) are shown by crosses. The curve changes into a steep exponential at 300 mv, due to the onset of storage capacitance. C_{tr} is extrapolated from the low-voltage data of Fig. 9 according to the law for an abrupt junction (see section D). For our purpose it is sufficiently accurate to use the form $C_{tr}=C_0/(600-V)^{\frac{1}{2}}$, with V the bias in millivolts. G_{th} is obtained from the G-V curve for the same diode by subtracting the excess current. All these quantities are plotted in Fig. 9; the dashed line is an arbitrary reference with slope e/kT. To the limited accuracy of the data, it seems that the conductance and the capacitance are indeed due to minority carrier diffusion. This gives an approximate storage lifetime of 3×10^{-9} sec.

In Table II we list the values of lifetime [Eq. (7)] of our four diodes, and of two others measured by R. Cohen with a slotted line at frequencies between 400 and 2000 Mc/sec.[36] These data are plotted in Fig. 10. In spite of the rather large scatter of the points, they appear to fall into two groups. The position of the groups suggests, either that the lifetime is independent of doping or that the lifetime in the diode with Ga regrown is longer than in those with Pb-Sn-As regrown layers.

The only studies of lifetime in highly doped materials with which to compare our data were made by Kalashnikov *et al.*,[37] and Alekseeva *et al.*[38] who studied P-, Sb-, and Ga-doped germanium with 10^{17} carriers/cm^3. They found approximately the same value for all these hydrogenic impurities, shown by the square in Fig. 10. These authors, however, did not find the expected variation of lifetime with doping, and so concluded that the recombination was controlled by centers other than the dopant. As they point out, if recombination were via neutral donors or acceptors, then in nondegenerate materials the lifetime should vary as the reciprocal of the square of the concentration. This rule will not be precisely followed when the material is degenerate, but it serves as a rough extrapolation law to intercompare the measurements. The solid lines in Fig. 10 have the slope corresponding to a $1/n^2$ dependence of lifetime. The lifetimes in our diodes with As base do

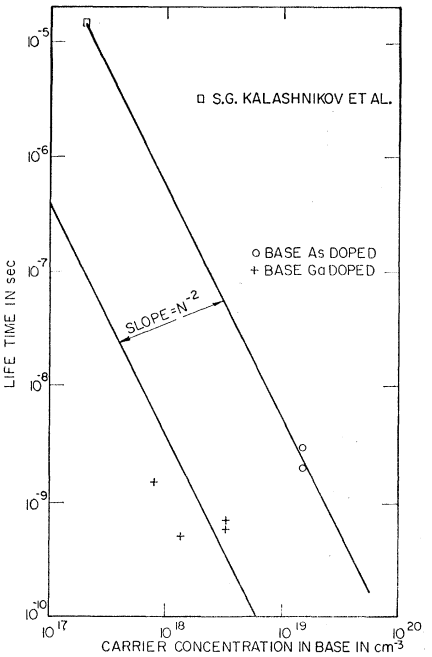

FIG. 10. Minority carrier capacitance deduced from storage admittance against doping in base. The solid lines are drawn with the slope corresponding to an n^{-2} dependence of lifetime. The square is from Kalashnikov *et al.*[37,38]

seem to be related to their P-, Sb-, and Ga-doped material, although the conclusion is most tentative because of the order-of-magnitude uncertainty in our values.

It is now possible to evaluate Eq. (6) for $T=300°$K, using the lifetimes defined by the solid lines in Fig. 10. The calculated values of $\phi=E_G+\zeta_{min}$ and E_G are given in Table II. In most cases either electron or hole current was found to be dominant, but in the more symmetrical junctions the separation was not clear. In the latter cases a spread of values is indicated in Table II. In addition, we estimate an uncertainty of ±50 mv contributed by the lifetime and V_{2000}.

The values of energy gap in the low-doped diodes appear to be close to the quantity in the pure material. In the more heavily doped diodes there may be a reduction in the height of the energy gap, but this reduction is less than the uncertainty in the calculations and no definite conclusions can be drawn. An approximately similar result has been obtained on one diode by Pankove.[30]

C. Excess Current

Exponential Excess Current

The excess current is composed of a number of components, of which we have studied mainly the one identified by the exponential increase of current with voltage. A typical example of the I-V characteristic

[36] R. Cohen (private communication). These measurements were of particular importance because the ratio of conductance to capacitance had the behavior with frequency expected for the region where the frequency and reciprocal lifetime are comparable (reference 12). We wish to thank Mr. Cohen for permission to present these unpublished data.

[37] S. G. Kalashnikov, E. Yu. L'vova, and V. V. Ostroborodova, J. Tech. Phys. (USSR) **27**, 1925 (1957) [translation: Soviet Phys.—Tech. Phys. **2**, 1789 (1957)].

[38] V. G. Alekseeva, I. V. Karpova, and S. G. Kalashnikov, Solid State Phys. (USSR) **1**, 529 (1959) [translation: Soviet Phys.—Solid State **1**, 475 (1959)].

at different temperatures is shown in Fig. 11.[39] The exponential excess current can be clearly seen in the low temperature characteristics. It extends from the current minimum to the thermal current region, a voltage range exceeding half the band gap. In some diodes, where the excess current is very low, the exponential increase may only be found at voltages just below the onset of the thermal current, or is not observed at all.

Chynoweth *et al.*[10] have quantitatively described the dependence of the exponential excess current on doping and on bombardment damage. Their model is based on a suggestion of Esaki[9] that this current is due to tunneling via impurity states in the forbidden gap. They express the exponential excess current density as

$$J_{\text{exc}}=D' \exp[-\beta' m^{*\frac{1}{2}} n^{*-\frac{1}{3}}(E_G-eV+Q)]. \quad (8)$$

The quantity Q is a function of the sum of the Fermi level penetrations, which is not explained but is small compared to E_G. D' is a function of V and represents the variation of the density of impurity states with energy within the forbidden gap. The form in which Eq. (8) is given shows the close relationship of the exponential tunneling factor to the band-to-band tunnel current, Eq. (4).

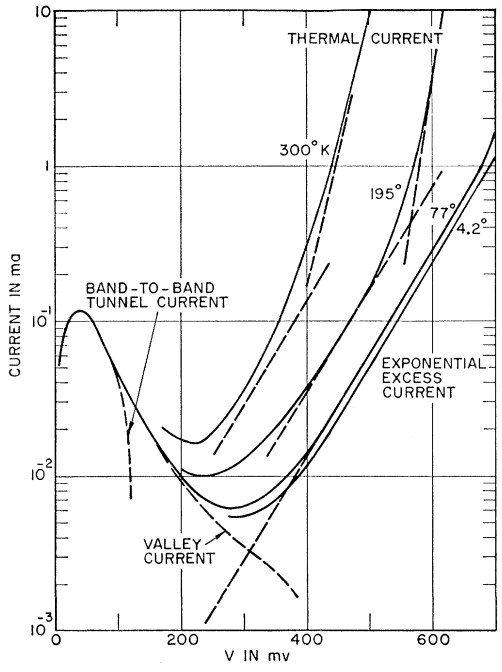

FIG. 11. Forward characteristic after correction for series resistance. The solid lines are measured; the dotted lines are a proposed decomposition into conduction processes. Diode T-1, In-½%Ga dot alloyed on As-doped wafer with 1.8×10^{19} electrons/cm³.

[39] Diode T-1, shown in Fig. 11, is not one of the solution grown diodes but an alloyed diode on an As doped wafer. The tunneling characteristics and method of fabrication indicate roughly symmetrical doping with $n^*=10^{19}/\text{cm}^3$. It is illustrated here because the excess current is particularly well defined. Other diodes show a similar behavior.

TABLE III. Exponential excess current at 4.2°K. The slope of the exponential curve, σ, is given by $\beta' m^{*\frac{1}{2}} n^{*-\frac{1}{3}}$ and the current density at 735 mv is equal to D' of Eq. (8).

Diode	Exponential slope (σ) (v^{-1})	Current density at 735 mv (amp/cm²)	$V(4.2°K)-V(300°K)$ at constant current (mv)
N-1-*A*	27.2	1100	175
N-1-*B*	21.5	900	150
N-1-*C*	24.2	700	155
N-2-*A*		300	
N-3-*A*	17.7	240	190
N-3-*B*	14.9	700	170
N-4-*A*	11.0	640	160
N-4-*B*	10.2	130	200
P-1-*A*	42	1500	
P-1-*B*	28	2000	200
P-3-*A*	26	3800	180
P-3-*B*	32	5000	
P-4-*A*	28	1600	180
P-6-*A*	20.4	1200	210
P-7-*A*			190

The measured values of the exponential slope ($\sigma=e\beta' m^{*\frac{1}{2}} n^{*-\frac{1}{3}}$) and of the constant D' at 4.2°K are listed in Table III. Since σ varies little with temperature, we have only tabulated it at 4.2°K where the accuracy is best. Figure 12 is the plot of σ against $n^{*-\frac{1}{3}}$; according to Eq. (8), it should yield a straight line through the origin with slope $e\beta' m^{*\frac{1}{2}}$. This is approximately the case although there is considerable scatter. The solid line shown is drawn with a slope $\beta' m^{*\frac{1}{2}} = 3.1\times10^{+10}$ ev^{-1} cm$^{-\frac{3}{2}}$, the value deduced from the change of peak current with doping, Fig. 4. Whether or not there is a significant difference between $\beta m^{*\frac{1}{2}}$ for band-to-band tunneling and $\beta' m^{*\frac{1}{2}}$ for excess current is not certain; in any case, the close agreement emphasizes the tunneling nature of the exponential excess current.

The temperature dependence of I_{exc} can be best expressed as the variation of V_I, the voltage at which the current reaches a fixed reference value, since σ is independent of temperature. If Eq. (8) applies, V_I will vary linearly with the energy gap ($eV_I-E_G=\text{const}$), providing D' is not temperature dependent. The experimental results are presented as $\Delta V_I=V_I(4.2°\text{K})-V_I(300°\text{K})$ in Table III. These values are all 2 to 3 times as large as the change of the energy gap: $E_G(4.2°\text{K})-E_G(300°\text{K})=76$ mev. The same result is found in the measurements of Chynoweth *et al.*[10] for Si. The constant D' must, therefore, be strongly temperature dependent, and this dependence is approximately independent of doping.

Discussion

Chynoweth *et al.* postulated a very specialized distribution of localized impurity states in the forbidden region to explain the exponential nature of the exponential excess current.[10] For D' (Eq. 8) to be voltage-independent, the states must have an energy distribution

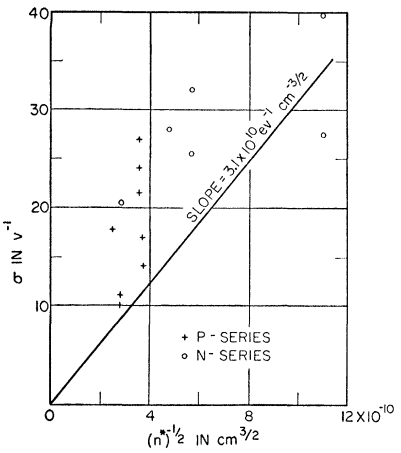

FIG. 12. Exponential excess current. Logarithmic derivative of current against reciprocal root of the reduced doping. The solid line is deduced from the data on the peak current.

independent of or varying exponentially with the energy, and this distribution must be maintained over a range of the gap as large as the voltage range of the excess current. For some of our germanium diodes (Fig. 11) this means for more than half the gap. A similar requirement applies to the silicon diodes of reference 10, and particularly to those radiation induced defects which increase the absolute value of the exponential excess current without changing its voltage dependence.[10,23] Such a distribution of localized states seems unlikely, in view of our present knowledge of impurity states in Ge and of the radiation induced defects in Si.[40] A somewhat different model of the excess current is discussed in II; it retains the formal structure of Eq. (8), but explains the voltage-independence of D' in a more natural way.

According to II, the term D' in Eq. (8) is determined by the recombination of a carrier in a tunneling state, and it is suggested that this interaction is similar to the recombination determining the thermal current and the carrier lifetime. The P diodes show that D' is independent of the gallium content in the base (the more lightly doped side); when the base is doped with arsenic, the value of D' seems to be appreciably smaller. For lack of knowledge as to which dopant serves as recombination center for the excess current, we do not try to correlate the value of D' with the minority carrier lifetime except to point out that both D' and τ seem to reflect a difference between N and P groups of diodes.

Hump Current

A second type of excess current, the hump current, is characterized by structure in the I-V curve beyond the current minimum. The shape is strongly temperature dependent. This current was first observed by Esaki[2,9] and explained as tunneling to localized impurity states. A number of authors have studied the hump current associated with various types of impurities.[20,23,41] Our diodes, which have no intentionally added impurities or defects, do not exhibit hump currents.

Valley Current

A third component of current which seems to be excess is the valley current. It can be observed clearly in junctions that have a well defined exponential excess current component, such as shown in Fig. 11, which can be extrapolated to lower voltage and subtracted from the I-V characteristic. The difference is the valley excess current, which joins smoothly onto the band-to-band tunnel current [Eq. (3)] and appears to be an extension of the latter. The valley current is nearly temperature independent. In heavily doped junctions the valley current increases faster than the exponential excess current, and the latter may disappear almost completely. An example is shown in Fig. 13.

A detailed study of the valley excess current was not possible because of the large extrapolation needed to deduce it from the I-V characteristic. Two associated quantities which can be measured are the peak-to-valley current ratio I_p/I_v and the voltage at the minimum V_v. These quantities are shown in Table IV for the P-diodes at 4.2°K, where the exponential excess and the thermal currents are smallest. In the less heavily doped diodes the exponential excess current was relatively large, which reduced the peak-to-valley ratio and shifted V_v to a much lower value. No quantitative data was taken on these because of the extreme variation in the valley current among diodes of the same group.

The one striking feature shown by Table IV is the constancy of the peak-to-valley ratio. From P-6 to

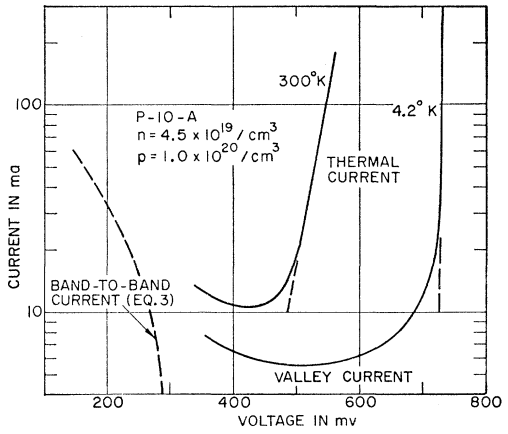

FIG. 13. Current-voltage characteristic near the valley. Heavily doped diode showing no exponential excess current. The data have been corrected for series resistance.

[40] For example, H. Y. Fan and A. K. Ramdas, J. Appl. Phys. **30**, 1127 (1959).

[41] N. Holonyak, Jr., J. Appl. Phys. **30**, 130 (1961); C. T. Sah, Phys. Rev. **123**, 1594 (1961); C. B. Purie, H. H. Sander, and A. D. Kantz, Bull. Am. Phys. Soc. **6**, 344 (1961).

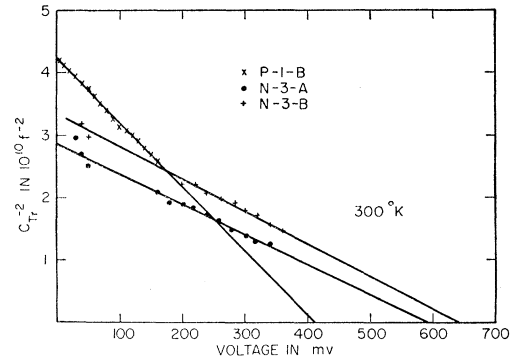

FIG. 14. Transition capacitance. Reciprocal capacitance squared vs voltage for three diodes. The intercept with the abscissa is the diffusion potential V_d.

P-9, the current density changes by a factor of 7 with no change in the current ratio. This indicates that the current in the valley is closely associated with the mechanism of the band-to-band tunnel current. The voltage at the minimum increases slowly with doping; the shift is less rapid than the increase in the sum of the Fermi level penetrations (Table IV).

It has been suggested[31] that the valley excess current is due to tunneling between tailing states,[42] which have been separated from the band edge by the heavy doping. This suggestion can readily account for the temperature-independence of the valley current and its persistence to voltages where the unperturbed bands have been uncrossed. However, the expected increase of the density of tailing states with doping should increase the valley current relative to the peak current, in contradiction to the behavior of diodes *P*-6 to *P*-9. No deduction has been made of the energy distribution of the tailing states needed to give the observed shape of the minimum, nor has their effect on the thermal current been discussed.

D. Transition Capacitance

Another determination of the band gap can be derived from measurements of the transition capacitance at low biases (Fig. 9). The diffusion potential V_D (Eq. 1) has the value $(E_G+\zeta_n+\zeta_p)$[6] in nondegenerate and $E_G+0.6(\zeta_n+\zeta_p)$ in degenerate material.[43] It is calculated from the extrapolation of the C^{-2} vs V plot. Although all our graphs give good straight lines (Fig. 14), this is not a proof that our junctions are indeed abrupt. In fact, we find nearly as good straight lines from plots of either C^{-1} or C^{-3} against V. We feel the C^{-2} plot is preferable, because the evaluation of the tunneling current indicates the junctions are essentially abrupt. Measured values of V_d are tabulated in Table V. They show no systematic variation, but are consistently lower than the predicted values. Such an effect has already been noted by Chynoweth *et al.*[4]

These unexpected values of V_D may be explained by assuming that the junction is not truly abrupt, i.e., there is an interdiffusion or overlap of donors and acceptors *within* the junction region. However, a low value of V_D means an *increased* net impurity concentration (donors minus acceptors) near the barrier, and it seems unlikely that an overlap of donors and acceptors will produce this.

Another possibility is that the simple theory no longer applies in these narrow junctions, where the impurity atoms can no longer be treated as uniformly distributed. However, low values of V_D are observed in such a variety of diodes that a more general explanation seems to be required.

TABLE IV. Valley current parameters at 4.2°K. Ratio of peak to valley current (I_p/I_v) and difference between valley voltage (V_v) and the sum of the Fermi penetrations ($\zeta_n+\zeta_p$).

Diode	I_p/I_v	$\zeta_n+\zeta_p$ (mv)	V_v (mv)	$V_v-(\zeta_n+\zeta_p)$ (mv)
P-6-*A*	29	158	470	290
P-6-*B*	25	158	430	
P-7-*A*	29	175	450	275
P-8-*A*	30	221	510	290
P-8-*B*	38	221	510	
P-8-*C*	30	221	510	
P-9-*B*	23	225	470	245
P-10-*A*	6.5	298	450	200
P-10-*B*	11.5	298	550	
P-11-*A*	14	329	550	200
P-11-*B*	9.5	329	500	
P-12-*A*	8.5	454	550	100
P-12-*B*	9.3	454	550	
P-12-*C*	5.4	454	550	

IV. CONCLUSION

The forward current in germanium tunnel diodes can be divided into a number of different regions according to the mechanism of current flow. The thermal current, which flows at large forward voltage, obeys the law

TABLE V. Diffusion potential barrier V_D [Eq. (10)] at 300°K determined from the intercept of the $1/C^2$ vs V curve.

Diode	V_D (mv)
N-3-*A*	589
N-3-*B*	638
N-4-*A*	589
N-4-*B*	594
P-1-*B*	405
P-2-*A*	510
P-3-*A*	552
P-3-*B*	528
P-3-*C*	545

[42] R. H. Parmenter, Phys. Rev. **104**, 22 (1956); M. Lax and J. C. Phillips, Phys. Rev. **110**, 41 (1958).
[43] C. T. Sah (private communication).

$J=J_0 \exp(eV/kT)$ within experimental error of $\pm 5\%$ at 300°K and $\pm 10\%$ at 195°K. At 77°K the exponent is 0.8 eV/kT $\pm 25\%$. The height of the barrier to current flow can be determined unambiguously at low temperatures; we find it is only a few millivolts less than the band gap of pure material. The spread of the impurity bands of the donors and acceptors may account for this shrinkage.

The lifetimes of the diodes which could be measured were around a nanosecond. The junction grown from a Pb-Sn-As solution has a larger recombination rate per doping atom than does the junction regrown from the In-Ga solution.

The exponential excess current, which is observed at voltages below the thermal current, follows the law $J=J_0' \exp(\sigma V)$ over a range of voltage which may exceed half the band gap. It appears to be closely related to the band-to-band tunnel current. The change of σ with doping and temperature is consistent with a model of indirect tunneling in which carrier energy is not conserved.

The band-to-band tunneling current with conservation of carrier energy is well described by Kane's theory for a direct transition.[8] The peak current density is in quantitative agreement with the prediction, and the location of the maximum is also accounted for except in very unsymmetrically doped junctions. Beyond the peak current the shape of the I-V characteristic deviates strongly from the theory. In particular the valley current perists 100 to 300 mv beyond the sum of the Fermi level penetrations, a region where the edges of the hands would be uncrossed. This valley excess current might be due to tunneling between tailing states which have been split off from the band edges by the impurities and the junction field. These states are presumably sufficiently localized to prevent their contributing to the conduction process in the bulk material. Otherwise they would have an effect on the barrier height for the thermal current, an effect which is not observed.

The change of tunnel current with temperature is positive for heavily doped junctions and negative for lightly doped ones. This is in agreement with the prediction that at high degeneracy the variation of the energy gap dominates, while at low degeneracy the change of Fermi level penetration with temperature is more important.

ACKNOWLEDGMENTS

The authors wish to express their gratitude to numerous members of the RCA Laboratories whose assistance made this study possible. Particular thanks go to H. Nelson and C. S. Bragnum for the solution growth of the junctions and for studies of area and doping, to C. W. Mueller and A. W. Fisher for fabricating the diodes, to W. W. Ho for preliminary measurements on some of the P-group diodes, and to J. Hilibrand for numerous discussions on instrumentation and on interpretation.